JOC The Journal of Organic Chemistry

Article

pubs.acs.org/joc

# Long-Range $^{1}H-^{15}N$ *J* Couplings Providing a Method for Direct Studies of the Structure and Azide−Tetrazole Equilibrium in a Series of Azido-1,2,4-triazines and Azidopyrimidines

Tatyana S. Shestakova,[†] Zakhar O. Shenkarev,[‡] Sergey L. Deev,*[,†] Oleg N. Chupakhin,[†,§] Igor A. Khalymbadzha,[†] Vladimir L. Rusinov,[†] and Alexander S. Arseniev[‡]

[†]Ural Federal University, 19 Mira Street, 620002 Ekaterinburg, Russia

[‡]Shemyakin-Ovchinnikov Institute of Bioorganic Chemistry, Russian Academy of Sciences, 16/10 Miklukho-Maklaya Street, 117997 Moscow, Russia

[§]I. Ya. Postovsky Institute of Organic Synthesis, Ural Branch of the Russian Academy of Sciences, 22 S. Kovalevskoy Street, 620219 Ekaterinburg, Russia

Supporting Information

**ABSTRACT:** The selectively $^{15}N$ labeled azido-1,2,4-triazine **2*A** and azidopyrimidine **4*A** were synthesized by treating hydrazinoazines with $^{15}N$-labeled nitrous acid. The synthesized compounds were studied by $^{1}H$, $^{13}C$, and $^{15}N$ NMR spectroscopy in DMSO, TFA, and DMSO/TFA solutions, where the azide−tetrazole equilibrium could lead to the formation of two tetrazoles (**T**, **T′**) and one azide (**A**) isomer for each compound. The incorporation of the $^{15}N$ label led to the appearance of long-range $^{1}H-^{15}N$ coupling constants ($J_{HN}$), which can be measured easily by using amplitude-modulated 1D $^{1}H$ spin−echo experiments with selective inversion of the $^{15}N$ nuclei. The observed $J_{HN}$ patterns enable the unambiguous determination of the mode of fusion between the azole and azine rings in the two groups of tetrazole isomers (**2*T′**, **4*T′** and **2*T**, **4*T**), even for minor isoforms with a low concentration in solution. However, the azide isomers (**2*A** and **4*A**) are characterized by the absence of detectable $J_{HN}$ coupling. The analysis of the $J_{HN}$ couplings in $^{15}N$-labeled compounds provides a simple and efficient method for direct NMR studies of the azide−tetrazole equilibrium in solution.

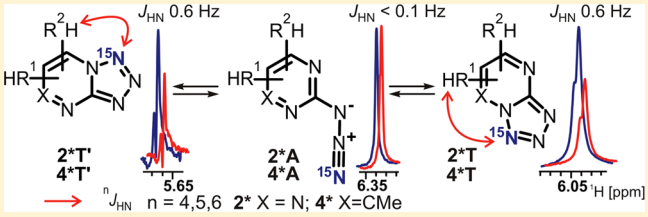


## INTRODUCTION

The wide range of photochemical and chemical properties of azidoazines has led to the broad applicability of these synthetic molecules in a variety of fields. For example, the azide−alkyne click chemistry reaction, which forms 1,2,3-triazole derivatives, is a new synthetic approach for designing both nucleoside analogues[1−3] and 1,2,3-triazolylpyridine ligands.[4,5] In addition, azidoadenosine derivatives are used as photoactive cross-linkers in molecular biology.[6−8] N-heterocycles that bear an azido group $\alpha$ to the nitrogen atom have azide−tetrazole tautomers, which result in the formation of fused tetrazoles; tetrazoles can be utilized as hetarylazides when they are in the closed form.[9−11] When the azido group attached to the azine ring between two nitrogen atoms (structure **A**) undergoes a cyclization, the formation of two differently fused tetrazoloazines, **T** and **T′** (Scheme 1), is possible. In this case, the elucidation of the isomeric tetrazole structure in solution is important because a shift in the equilibrium between the different isoforms (**A**/**T**/**T′**) may significantly influence the compound's activity. Similar isomeric properties are present in several classes of heterocyclic compounds. The annulation of azoles (i.e., imidazole, 1,2,3-triazole, 1,2,4-triazole and thiazole) to 1,2,4-triazines or pyrimidines via the carbon atom between two nitrogens of azine also leads to two possible azole ring cyclizations.[12−19] Furthermore, the Dimroth rearrangement of the azine ring may alter the type of fusion between the azole and azine rings.[20]

The ring−chain tautomerism in a series of azido-1,2,4-triazines **A** (X = N) and azidopyrimidines **A** (X = $CR^3$) was previously investigated by natural-abundance $^{1}H$ and $^{13}C$ NMR spectroscopy.[21−29] Although the equilibrium between azide (**A**) and tetrazole (**T** or **T′**) can be tracked via their $^{1}H$ and $^{13}C$ chemical shifts, the elucidation of the dominant tetrazole isomer structure (**T** or **T′**) in solution is not straightforward. For the indirect determination of the tetrazole structure, its $^{1}H$ and $^{13}C$ NMR spectra are compared with the data acquired for model compounds: e.g., deaza analogues.[25−27,29] The application of natural-abundance $^{15}N$ NMR spectroscopy to studies of the azide−tetrazole equilibrium in solvent-free samples of tetrazolo[1,5-*a*]pyrimidines (**A**, X = $CR^3$; Scheme 1) was also reported.[30] Although it is possible to obtain direct structural information about the different azide and tetrazole isoforms, the low sensitivity of natural-abundance $^{15}N$ NMR restricts the application of this approach to liquid substances.

**Received:** April 16, 2013
**Published:** June 10, 2013

   dx.doi.org/10.1021/jo4008207 | *J. Org. Chem.* 2013, 78, 6975−6982

**Scheme 1. Selective $^{15}N$ Labeling and Analysis of $J_{CN}$ or $J_{HN}$ Couplings Allowed for the Direct Study of the Azide−Tetrazole Equilibrium in the Series of Azido-1,2,4-triazines A (X = N) and 2-Azidopyrimidines A (X = CR$^3$)[a]**

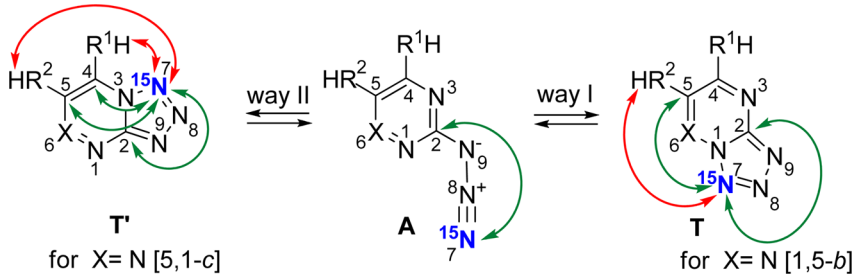


[a] $^{13}C-^{15}N7$ and $^{1}H-^{15}N$ *J*-coupling constants ($J_{CN}$ and $J_{HN}$) that were expected for the different isomers (**A**/**T**/**T′**) of azido-1,2,4-triazines (X=N) are highlighted with green and red arrows, respectively. The formation of the tetrazolo[1,5-*b*][1,2,4]triazines **T** (X=N) is identified by the $J_{CN}$ couplings for two $^{13}C$ nuclei (C2 and C5) and long-range $J_{HN}$ couplings for protons from $R^2$ substitution. Alternative structures **T′** (X=N) with [5,1-*c*] fusion should exhibit three $J_{CN}$ couplings (with C2, C4 and C5) and a long-range $J_{HN}$ for protons on the $R^1$ and $R^2$ substitutions. The azides **A** (X=N) are characterized by single $^{3}J_{C2-N7}$ coupling and the absence of detectable $J_{HN}$. The different isomers (**A**/**T**/**T′**) of azidopyrimidines (X=CR$^3$) also can be distinguished by $J_{CN}$ or $J_{HN}$ patterns.

The selective incorporation of $^{15}N$ atoms into the azole fragment of a tetrazoloazine significantly facilitates the direct NMR studies of the azide−tetrazole equilibrium in solution.[31−33] In this case, the chemical shift of $^{15}N$ nuclei may distinguish the cyclic form from the open form of the azidoazine. Recently, we have demonstrated that selective $^{15}N$ labeling of the azole ring, when followed by the analysis of $^{13}C-^{15}N$ ($J_{CN}$) coupling constants, facilitates the unambiguous elucidation of the tetrazole isomer structures **T** and **T′** (Scheme 1).[34] However, the limited sensitivity of natural-abundance $^{13}C$ spectroscopy significantly hindered the application of $J_{CN}$ analysis to studies of isomeric forms that have a low concentration in solution. Therefore, a more sensitive spectroscopic method, which permits the structural determination of mixtures of several isomers, is highly desirable for direct studies of the azide−tetrazole equilibrium. By using known examples of $^{15}N$-labeled azidobenzo-1,2,4-triazine **A** (X = N, Scheme 1) and 2-azidopyrimidine **A** (X = CR$^3$, Scheme 1), we report that the quantitative characterization of the long-range $^{1}H-^{15}N$ *J* couplings ($J_{HN}$) provides a simpler and more efficient method for the study of the azide−tetrazole equilibrium in solution. In the current study, the data obtained from the analysis of the $J_{HN}$ couplings are compared with the $J_{CN}$ patterns measured for the mixtures of different isomers (**A**/**T**/**T′**) of these compounds. This proposed method facilitates the straightforward determination of the tetrazole isomer structures, even when the $J_{CN}$ couplings could not be measured due to the insufficient sensitivity of natural-abundance $^{13}C$ NMR.

## RESULTS AND DISCUSSION

The incorporation of a $^{15}N$ label at position 7 of the azido-1,2,4-triazine was performed according to a previously described protocol.[34] The reaction between heteroarylhydrazine **1** and $^{15}N$-nitrous acid, which was generated with acetic acid and $Na^{15}NO_2$ (98% $^{15}N$), yielded compound **2*A**, which had 98% $^{15}N$ enrichment (Scheme 2). The same procedure was used to incorporate a $^{15}N$ atom into 2-azidopyrimidine. The reaction between 2-hydrazinopyrimidine **3** and $^{15}N$-enriched nitrous acid produced azide **4*A** with 86% $^{15}N$ enrichment (Scheme 3). In this case, $^{15}N$-nitrous acid was generated from $K^{15}NO_2$ (86% $^{15}N$).

The synthesized compounds were studied by $^{1}H$, $^{13}C$, and $^{15}N$ NMR spectroscopy in DMSO, TFA, and mixtures of these

**Scheme 2. Synthesis of Selectively $^{15}N$ Labeled 2* and the Associated NMR $J_{CN}$ Data That Confirm the Structure of the Azide (A) and Tetrazole (T and T′) Isomers[a]**

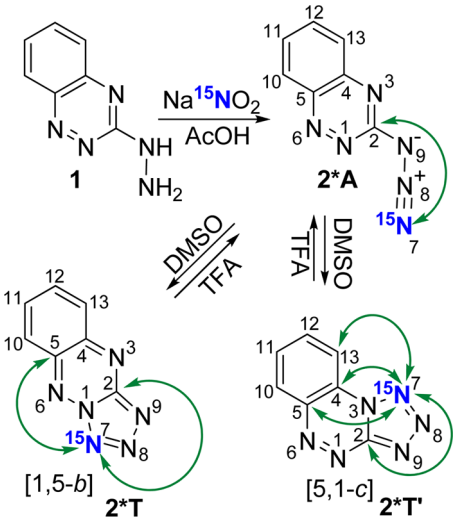


[a] The azide−tetrazole equilibrium is shifted to the tetrazole/azide forms in the DMSO/TFA solutions, respectively. The observed $J_{CN}$ couplings with the $^{15}N7$ nucleus are indicated by green arrows. The detection limit of the $J_{CN}$ measurement was 0.3 Hz.

solvents (Table 1, Figures 1A,B and 2A,B). Selective $^{15}N$ labeling of compounds **2*** and **4*** resulted in the appearance of $^{13}C-^{15}N$ and $^{1}H-^{15}N$ heteronuclear spin−spin interactions. The $J_{CN}$ couplings (Table 2) were detected and measured using previously described methods.[34] The $J_{HN}$ values (Table 3) were measured quantitatively by using amplitude-modulated 1D $^{1}H$ spin−echo experiments that were acquired with and without the selective inversion of the $^{15}N$ nuclei (Figures 1C and 2C).[34,35]

Three sets of signals with relative intensities of 79/12/9 were observed in the $^{1}H$, $^{15}N$, and $^{13}C$ NMR spectra of azidotriazine **2*** in DMSO (Figure 1A,B and Figure S1 in the Supporting Information). The two $^{15}N$ signals with chemical shifts (−35.5 and −31.0 ppm) characteristic of fused tetrazoloazines[32,33] most likely correspond to the N7 of the two tetrazole isomers (**2*T′** and **2*T**). The third nitrogen signal (−140.3 ppm) potentially belonged to the N7 of azidoazine **2*A**. The $J_{HN}$ and


dx.doi.org/10.1021/jo4008207 | J. Org. Chem. 2013, 78, 6975−6982

**Scheme 3. Synthesis of Selectively $^{15}$N Labeled 4* and Associated NMR $J_{CN}$ Data That Confirm the Structures of the Azide (A) and Tetrazole (T and T′) Isomers**[a]

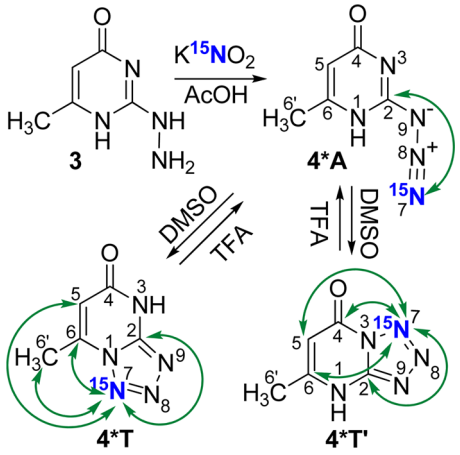


[a]The azide-tetrazole equilibrium is shifted to the tetrazole/azide forms in the DMSO/TFA solution, respectively. The observed $J_{CN}$ couplings with the $^{15}$N7 nucleus are indicated by green arrows. The detection limit of the $J_{CN}$ measurement was 0.3 Hz.

**Table 1. Azide−Tetrazole Isomerization of the Studied Compounds in Different Solvents**

| compd | solvent | T′/A/T |
|---|---|---|
| **2*A** | DMSO | 79/12/9[a] |
| | DMSO/TFA (9/1) | 75/13/12 |
| | DMSO/TFA (3/1) | 70/19/11 |
| | TFA | 1/99/0 |
| **4*A** | DMSO[b] | 8/0/92[c] |
| | DMSO[d] | 51/0/49[e] |
| | DMSO/TFA (3/1) | 49/0/51 |
| | DMSO/TFA (1/1) | 47/2/51 |
| | DMSO/TFA (2/3) | 24/29/47 |
| | TFA | 0/96/4[f] |

[a]The 65/25/10 concentration ratio of **2T′/2A/2T** in DMSO solution was reported previously.[29] [b]After dissolution. [c]Only **4T** isomer was previously observed directly after dissolving **4A** in DMSO.[22] [d]Twenty-four hours after dissolution at 30 °C. [e]The 48/52 concentration ratio of **4T′/4T** in DMSO solution at 100 °C was observed previously 5 h after dissolution.[22] [f]**4T** isomer was previously not observed in TFA solution.[22]

$J_{CN}$ values revealed that the major isomer of the compound was **2*T′** (Schemes 2 and 4). The spin−spin interactions that were detected between the N7 and the protons, H13 ($^4J_{HN} \approx 0.16$ Hz) and H10 ($^5J_{HN} \approx 0.11$ Hz), were only consistent with the [5,1-*c*] type of fusion between the tetrazole and 1,2,4-triazine rings. This result was also supported by the observation of the $J_{CN}$ values for C2, C4, C5, and C13 (Table 2). Interestingly, smaller $J_{HN}$ values were measured for the other protons in the **2*T′** benzo ring ($^5J_{H12-N7}$ and $^6J_{H11-N7} \approx 0.04$ Hz). The corresponding cross-peaks at the $^{15}$N7 (**2*T′**) frequency were also observed in the 2D $^{15}$N-HMBC spectrum (Figure S2 in the Supporting Information). Concurrently, due to the different relaxation properties of the protons and the presence of homonuclear $^1$H−$^1$H spin−spin couplings, the intensities of HMBC cross-peaks were not correlated with the amplitude of $J_{HN}$.

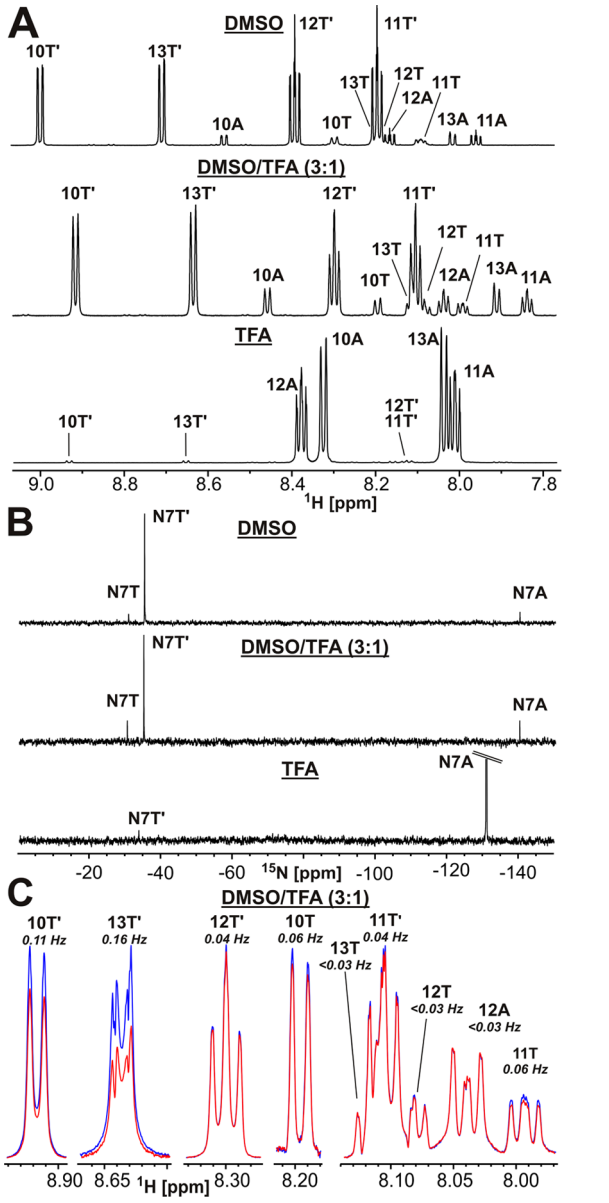


**Figure 1.** NMR analysis of **2*T**, **2*T′**, and **2*A** in different solvents: (A, B) 1D $^1$H and $^{15}$N spectra in DMSO-$d_6$, TFA-*d*, and a DMSO-$d_6$/TFA-*d* (3/1) mixture; (C) fragments of 1D $^1$H amplitude modulated spin−echo spectra measured with selective inversion of $^{15}$N7T and $^{15}$N7T′ (red) or $^{15}$N7A (blue) nuclei. The spectra were measured in a DMSO-$d_6$/TFA-*d* (3/1) mixture using a spin−echo delay (delay for evolution of $J_{HN}$) of 2 s. The spectral fragments are presented in absolute value mode to exclude the phase distortions created by the homonuclear $^1$H−$^1$H *J* couplings. The measured $J_{HN}$ values are shown in Table 3. The signals marked with the label "<0.03 Hz" do not exhibit any $J_{HN}$ couplings within the detection limit.

The observed broadening of the $^1$H, $^{13}$C, and $^{15}$N resonances of the minor tetrazole form (**2*T**) revealed the presence of a chemical exchange process between the tetrazole and azide isomers in the DMSO solution. This prevents the measurement of the $J_{HN}$ and $J_{CN}$ couplings. The addition of TFA to the DMSO solution led to an increase in the relative concentration of the minor forms and to a significant narrowing of the **2*T** resonances (Figure 1A,B). These results are caused by the TFA-induced protonation of the nitrogen atoms in the azine and tetrazole moieties, which is associated with changes in the


dx.doi.org/10.1021/jo4008207 | J. Org. Chem. 2013, 78, 6975−6982

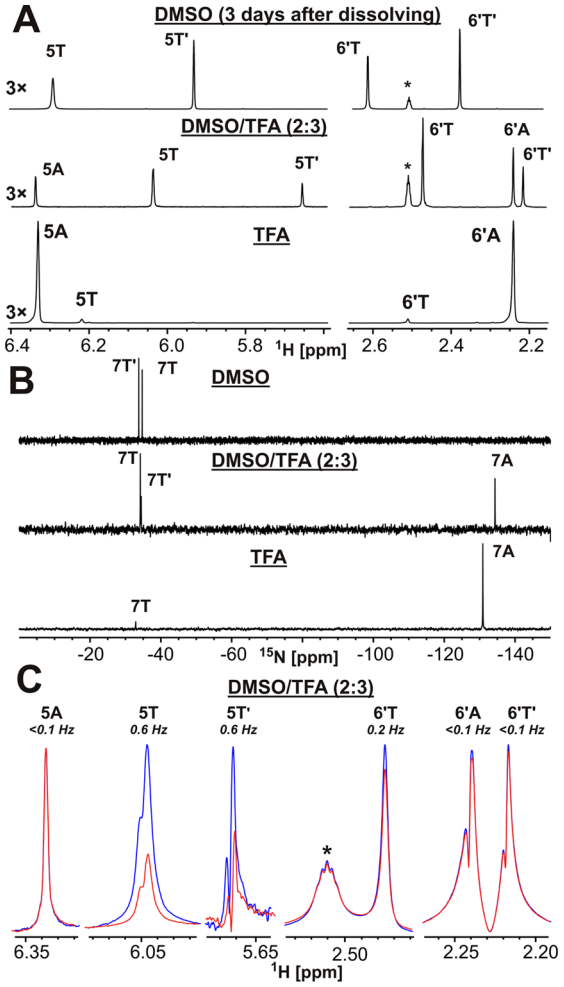


**Figure 2.** NMR analysis of **4*T**, **4*T′** and **4*A** in different solvents: (A, B) 1D $^{1}$H and $^{15}$N spectra in DMSO-$d_6$, TFA-*d*, and a DMSO-$d_6$/TFA-*d* (2/3) mixture (the intensity of the downfield spectral fragments in (A) is increased 3-fold.); (C) fragments of 1D $^{1}$H amplitude-modulated spin−echo spectra measured with selective inversion of $^{15}$N7T and $^{15}$N7T′ (red) or $^{15}$N7A (blue) nuclei. The spectra were measured in a DMSO-$d_6$/TFA-*d* (2/3) mixture using spin−echo delay (delay for evolution of $J_{HN}$) of 0.6 s. The spectral fragments are presented in absolute value mode to exclude phase distortions originated by homonuclear $^{1}$H−$^{1}$H *J* couplings. The measured $J_{HN}$ values are shown in Table 3. The signals marked with the label "<0.1 Hz" indicate that no $J_{HN}$ couplings were observed within the detection limit. The residual $^{1}$H signal of DMSO is marked with an asterisk.

isomerization rates between the different isoforms.[34] The $J_{HN}$ and $J_{CN}$ couplings for **2*T** and **2*A** were subsequently measured at 10 or 25% TFA in DMSO (Figure 1C). The observed spin−spin interactions between N7 and the protons H10 ($^{5}J_{HN} \approx 0.06$ Hz) and H11 ($^{6}J_{HN} \approx 0.06$ Hz), in addition to the $J_{CN}$ that was detected for the C2 and C5 carbons, confirmed the formation of the [1,5-*b*] fusion between the tetrazole and 1,2,4-triazine rings in isomer **2*T** (Schemes 2 and 4). As expected, azide isomer **2*A** was characterized by the absence of a detectable $J_{HN}$ coupling, as well as a single $^{3}J_{C2-N7}$ coupling with a magnitude of ∼0.4 Hz.

In pure TFA, compound **2*** underwent almost complete rearrangement to yield open-chain azide isomer **2*A** (Figure 1A,B) characterized by the single $^{3}J_{C2-N7}$ (∼0.6 Hz), the absence of detectable $J_{HN}$, and a $^{15}$N7 signal (−130.9 ppm) in the chemical shift range typical for azidoazines.[32,33] The minor tetrazole isomer ($\delta(^{15}N7)$ −33.9 ppm) was also observed in TFA. The low concentration (∼1%) of this form precluded the direct observation of its $^{13}$C signals and $J_{CN}$ measurements. Nevertheless, the measured $^{4}J_{H13-N7}$ and $^{5}J_{H10-N7}$ couplings (∼0.17 and 0.13 Hz, respectively) confirmed the formation of the tetrazole **2*T′** structure with the [5,1-*c*] type of fusion between the azole and azine rings (Scheme 4). It should be noted that the $J_{HN}$ and $J_{CN}$ values measured for the **2*A** and **2*T′** isomers in different solvent systems were identical within the experimental error range.

Two sets of signals that corresponded to the two tetrazole isomers were observed in the $^{1}$H, $^{15}$N, and $^{13}$C NMR spectra of sample **4*** in DMSO (Figure 2A,B and Figure S7 in the Supporting Information). The relative concentrations of the **4*T** and **4*T′** isomers ($\delta(^{15}N7)$ −34.7 and −33.8 ppm, respectively) were 92/8 after dissolution of the substance and were transformed to approximately a 1/1 ratio after 24 h at 30 °C. The measured long-range $J_{HN}$ couplings confirmed the **4*T** and **4*T′** structures for the tetrazolo[1,5-*a*]pyrimidines (Scheme 4 and Table 3). For **4*T**, the spin−spin interactions with N7 were detected for the protons on the H6′ methyl group ($^{4}J_{HN} \approx 0.2$ Hz) and H5 ($^{4}J_{HN} \approx 0.6$ Hz), which indicated that the cyclization of the tetrazole ring via the N1 atom had occurred. The **4*T′** structure, which was fused at the N3 atom, was characterized by a single $^{4}J_{H5-N7}$ (∼0.6 Hz), as well as the absence of a detectable H6′−N7 interaction (associated $^{6}J_{HN} < 0.1$ Hz, Figure 2C). These results are in good agreement with the results of the 2D $^{15}$N-HMBC experiment (Figure S5 in the Supporting Information). The $^{13}$C−$^{15}$N spin−spin interactions that were detected for C2, C4, C5, and C6 validated the structure of the **4*T′** isomer. The exchange-induced broadening of the **4*T** signals only allowed the measurement of the $J_{CN}$ couplings for the C6 and C6′ nuclei. However, these data were sufficient to confirm that the tetrazole cyclization occurred via the N1 atom.

Similar to the situation observed for compound **2***, the addition of TFA to the DMSO solution strongly influenced the chemical exchange processes between the different isomers of **4***. In this case, a significant narrowing of the **4*T** resonances was observed with the addition of 25% TFA, but the azide **4*A** isomer ($\delta(^{15}N7)$ −134.4 ppm) only became detectable by NMR at more than 50% TFA addition (Figure 2B). Analysis of the $J_{HN}$ and $J_{CN}$ couplings conducted at 60% TFA validated the structures of the cyclic tetrazoles (**4*T**, **4*T′**) and azide **4*A** (Scheme 3 and Figure 2C). The small-amplitude $^{3}J_{C2-N7}$ coupling for azide **4*A** was not detected due to a drop in sensitivity that was caused by the dilution of the sample with TFA. Therefore, the azidopyrimidine structure of **4*A** was characterized by the absence of detectable $J_{HN}$ (>0.1 Hz) and $J_{CN}$ (>1 Hz) couplings.

The 96/4 mixture of the open-chain **4*A** ($\delta(^{15}N7)$ −131.0 ppm) and cyclic **4*T** ($\delta(^{15}N7)$ −32.9 ppm) isomers was observed upon the solubilization of azidopyrimidine **4*** in the TFA (Figure 2A,B). The low concentration of **4*T** did not permit the measurement of $J_{CN}$. However, the measured $^{4}J_{H5-N7}$ (∼0.7 Hz) and $^{4}J_{H6'-N7}$ (∼0.2 Hz) couplings validated that the formation of a tetrazole structure cyclized via the N1 atom had occurred (Schemes 3 and 4). These values were in good agreement with the observed results for **4*T** in DMSO (see above). As expected, the **4*A** isomer was characterized by a single $^{3}J_{C2-N7}$ coupling (∼0.6 Hz) and the absence of any detectable $J_{HN}$ interactions.


dx.doi.org/10.1021/jo4008207 | J. Org. Chem. 2013, 78, 6975−6982

Table 2. $^{13}C$ Chemical Shifts (ppm) and $^{13}C-^{15}N7$ $J$ Coupling Constants (Hz) of the Studied Compounds[a]

| compd | solvent | C2 | C4 | C5 | C6/C10 | other signals |
|---|---|---|---|---|---|---|
| **2*A** | DMSO | 159.18 | 141.56 | 145.56 | 129.86 | 130.79 (C11), 138.11 (C12), 127.69 (C13) |
| | DMSO/TFA (9/1) | 159.16 ($^3J_{CN}$ = 0.4) | 141.55 | 145.55 | 129.75 | 130.56 (C11), 137.85 (C12), 127.59 (C13) |
| | DMSO/TFA (3/1) | 159.14 | 141.54 | 145.51 | 129.57 | 130.18 (C11), 137.44 (C12), 127.43 (C13) |
| | TFA | 154.98 ($^3J_{CN}$ = 0.6) | 148.64 | 142.27 | 130.17 | 134.49 (C11), 146.34 (C12), 126.62 (C13) |
| **2*T**[b] | DMSO | ND[c] | 147.65[d] | ND | 127.69[e] | 135.31 (C11), 137.99 (C12), 129.22 (C13) |
| | DMSO/TFA (9/1) | 148.54[d] ($^2J_{CN}$ = 3.2) | 147.60 | 141.80 ($^3J_{CN}$ = 1.2) | 127.56 | 135.18 (C11), 137.86 (C12), 129.13 (C13) |
| | DMSO/TFA (3/1) | 148.42[d] | 147.51 | 141.71 | 127.35 | 134.93 (C11), 137.57 (C12), 128.99 (C13) |
| **2*T′**[b] | DMSO | 153.23 ($^2J_{CN}$ = 2.2) | 122.82 ($^2J_{CN}$ = 2.6) | 140.15 ($^3J_{CN}$ = 0.6) | 131.72 | 130.99 (C11), 138.32 (C12), 116.07 (C13) ($^3J_{C13-N7}$ = 0.6) |
| | DMSO/TFA (9/1) | 153.18 | 122.72 | 140.10 | 131.66[d] | 130.87 (C11,) 138.19 (C12), 115.95[d] (C13) |
| | DMSO/TFA (3/1) | 153.06 ($^2J_{CN}$ = 2.2) | 122.54 ($^2J_{CN}$ = 2.8) | 140.00 ($^3J_{CN}$ = 0.6) | 131.56[d] | 130.65 (C11), 137.92 (C12), 115.74 (C13) ($^3J_{C13-N7}$ = 0.6) |
| **4*A**[f] | DMSO/TFA (2/3) | 157.26 | 173.55 | 103.81 | 160.73 | 17.54 (C6′) |
| | TFA | 157.61 ($^3J_{CN}$ = 0.6) | 173.10 | 102.86 | 160.84 | 16.91 (C6′) |
| **4*T** | DMSO | 150.98[d] | 161.27[d] | 109.10[d] | 145.31[d] ($^2J_{CN}$ = 3.4) | 16.33 (C6′) ($^3J_{C6'-N7}$ = 0.8) |
| | DMSO/TFA (3/1) | 150.78 ($^2J_{CN}$ = 2.7) | 160.99[d] | 108.91 ($^3J_{CN}$ = 0.7) | 145.06 ($^2J_{CN}$ = 3.4) | 15.77 (C6′) ($^3J_{C6'-N7}$ = 0.8) |
| | DMSO/TFA (2/3) | 149.64 | 161.58 | 108.15 | 146.15 | 14.99 (C6′) |
| | TFA | ND | ND | 108.34 | 148.31 | 14.35 (C6′) |
| **4*T′**[b] | DMSO | 151.53 ($^2J_{CN}$ = 2.4) | 154.38 ($^2J_{CN}$ = 2.1) | 98.66 ($^3J_{CN}$ = 0.8) | 154.96 ($^4J_{CN}$ = 0.4) | 19.27 (C6′) |
| | DMSO/TFA (3/1) | 151.31 ($^2J_{CN}$ = 2.4) | 154.24 ($^2J_{CN}$ = 2.1) | 98.39 ($^3J_{CN}$ = 0.8) | 154.54[d] ($^4J_{CN}$ = 0.4) | 18.65 (C6′) |
| | DMSO/TFA (2/3) | 150.59 | 154.47 | 98.32 | 154.70[d] | 17.90 (C6′) |

[a] $^{13}C-^{15}N7$ $J$ coupling constants ($J_{CN}$) were measured using either $^{13}C$ line-shape analysis or amplitude-modulated spin−echo experiments. The experimental error in the measured $J_{CN}$ values was 0.15 Hz. $^{13}C$ chemical shifts were referenced indirectly relative to the proton signal of tetramethylsilane (TMS). [b] $^{13}C$ signals of the compound were not observed in TFA. [c] ND denotes that the signal was not observed due to the low concentration of the corresponding isomer. [d] The signal demonstrated additional broadening or splitting, which was not connected with the $J_{CN}$ or $J_{CH}$ couplings. [e] The signal overlapped with the C11 signal from compound **2*A**. [f] Signals for the compound were not observed in DMSO or in DMSO/TFA (3/1).

Therefore, we demonstrated that the selective $^{15}N$ labeling, when followed by the analysis of long-range $^1H-^{15}N$ $J$ couplings, can be effectively employed to study the azide−tetrazole equilibrium in azidoazines when the azide form **A**, in addition to both tetrazole isomers **T** and **T′**, is present in solution. This proposed approach complements the previously reported method, which was based on the analysis of $^{13}C-^{15}N$ $J$ couplings.[34] The enhanced sensitivity that was provided by the $^1H$ NMR (32-fold compared to direct $^{13}C$ detection) permits the precise measurement of $J_{HN}$ values with amplitudes as small as 0.1 Hz, even for cases where the direct registration of the $^{13}C$ resonances is problematic because the concentrations of the minor isomers are low. In contrast to those for $J_{CN}$, the $J_{HN}$ measurements require much less experimental time (minutes vs hours) and can be performed by using a conventional NMR instrument that is equipped with a double-resonance probe. The use of a direct method is indispensable for the determination of molecular structures, especially for compounds that may chemically rearrange in solution. For example, in the X-ray structure of **4**, only one tetrazole isomer, **4T**, was observed (Figure 3). However, according to the NMR analysis, the equilibrium state of the compound is composed of mixtures of three isoforms (**T**, **T′**, and **A**), whose relative concentration depends on the solvent properties.

Previously, the structures of **2** and **4** tetrazole isomers were studied by indirect UV−vis as well as $^1H$ and $^{13}C$ NMR spectroscopic methods that were based on comparisons with model compounds, which included the deaza analogues (tetrazoloisoquinolines, 1,2,4-triazolo[3,4-*c*]benzo-1,2,4-triazines) of tetrazolo[5,1-*c*][1,2,4]triazine **2T′**[29] and the N3-methyl derivative of **4**.[22] Although the structure of tetrazolo-[1,5-*b*][1,2,4]triazines (**T**, Scheme 1) is considered to be more energetically favorable than the [5,1-*c*] isomer (**T′**),[23] the formation of azoloazine **T′** with the [5,1-*c*] fusion was reported for the cyclization of azide **2A**.[29] Our re-examination of the azide−tetrazole tautomerism of **2*** that was conducted by using direct NMR methods confirms that cyclization of azide-1,2,4-triazines **A** can yield the unexpected tetrazolo[5,1-*c*][1,2,4]-triazines **T′**.[21,23,25−27,34]

The application of long-range $J_{HN}$ couplings for the characterization of nitrogen-containing heterocycles at a natural $^{15}N$ abundance was proposed approximately three decades ago.[36] The sensitivity enhancement that was provided by selective $^{15}N$ labeling allowed us to extend the applicability of


dx.doi.org/10.1021/jo4008207 | J. Org. Chem. 2013, 78, 6975−6982

**Table 3. $^{1}H$ and $^{15}N$ Chemical Shifts (ppm) and $^{1}H-^{15}N7$ $J$ Coupling Constants (Hz) of the Studied Compounds**

| | | | $\delta(^{1}H)^{b}$ | | | |
|---|---|---|---|---|---|---|
| compd | solvent | $\delta(^{15}N)^{a}$ | H10/H5 | H11/H6′ | H12 | H13 |
| **2*A** | DMSO | −140.3 (N7) | 8.56 | 7.96 | 8.17 | 8.02 |
| | DMSO/TFA (9/1) | −140.3 (N7) | 8.52 | 7.92 | 8.12 | 7.98 |
| | DMSO/TFA (3/1) | −140.2 (N7) | 8.46 | 7.84 | 8.04 | 7.91 |
| | TFA | −130.9 (N7), 3.4 (N6), −110.7 (N3) | 8.33 | 8.01 | 8.38 | 8.04 |
| **2*T**[c] | DMSO | −31.0 (N7)[d] | 8.30[d] | 8.09[d] | 8.20[e] | 8.20[e] |
| | DMSO/TFA (9/1) | −30.9 (N7) | 8.26 | 8.06 | 8.15[e] | 8.17[e] |
| | DMSO/TFA (3/1) | −30.6 (N7) | 8.19 ($^{5}J_{HN}$ = 0.06) | 7.99 ($^{6}J_{HN}$ = 0.06) | 8.08[e] | 8.11[e] |
| **2*T′** | DMSO | −35.5 (N7), −312.9 (N6), −155.7 (N3) | 9.00 ($^{5}J_{HN}$ = 0.11) | 8.20 ($^{6}J_{HN}$ = 0.04) | 8.39 ($^{5}J_{HN}$ = 0.04) | 8.71 ($^{4}J_{HN}$ = 0.15) |
| | DMSO/TFA (9/1) | −35.4 (N7) | 8.97 | 8.17 | 8.36 | 8.69 |
| | DMSO/TFA (3/1) | −35.3 (N7) | 8.92 ($^{5}J_{HN}$ = 0.11) | 8.10 ($^{6}J_{HN}$ = 0.04) | 8.30 ($^{5}J_{HN}$ = 0.04) | 8.64 ($^{4}J_{HN}$ = 0.16) |
| | TFA | −33.9 (N7) | 8.93 ($^{5}J_{HN}$ = 0.13) | 8.13 ND[f] | 8.13 ND[f] | 8.65 ($^{4}J_{HN}$ = 0.17) |
| **4*A**[g] | DMSO/TFA (2/3) | −134.4 (N7) | 6.34 | 2.24 | | |
| | TFA | −131.0 (N7), −228.6 (N1), −159.6 (N3) | 6.33 | 2.24 | | |
| **4*T** | DMSO | −34.7 (N7), −155.5 (N1) | 6.30[d] ($^{4}J_{HN}$ = 0.6) | 2.62 ($^{4}J_{HN}$ = 0.2) | | |
| | DMSO/TFA (3/1) | −34.8 (N7) | 6.17 | 2.56 | | |
| | DMSO/TFA (2/3) | −34.2 (N7) | 6.05 ($^{4}J_{HN}$ = 0.6) | 2.47 ($^{4}J_{HN}$ = 0.2) | | |
| | TFA | −32.9 (N7), −154.9 (N1) | 6.22 ($^{4}J_{HN}$ = 0.7) | 2.51 ($^{4}J_{HN}$ = 0.2) | | |
| **4*T′**[c] | DMSO | −33.8 (N7), −259.0 (N1), −136.9 (N3) | 5.94 ($^{4}J_{HN}$ = 0.6) | 2.38 | | |
| | DMSO/TFA (3/1) | −33.8 (N7) | 5.81 | 2.33 | | |
| | DMSO/TFA (2/3) | −34.5 (N7) | 5.67 ($^{4}J_{HN}$ = 0.6) | 2.22 | | |

[a] $^{15}N$ chemical shifts were referenced indirectly relative to nitromethane ($MeNO_2$). The chemical shifts of the $^{15}N7$ signals were measured in 1D $^{15}N$ spectra. The assignments of the other signals were obtained at natural $^{15}N$ abundance by using 2D $^{1}H$, $^{15}N$ HMBC spectra. [b] The $^{1}H-^{15}N7$ $J$ coupling constants ($J_{HN}$) were measured by using amplitude modulated spin−echo experiments. The spin−echo delays (delays for evolution of $J_{HN}$) were set to 2.0 and 0.6 s for compounds **2*** and **4***, respectively. The experimental errors in the measured $J_{HN}$ values were 0.02 and 0.05 Hz, respectively. [c] Signals of the compound were not observed in TFA. [d] The signal was broadened. [e] The signal overlapped with the H11 signal from compound **2*T′**. [f] Not determined, due to overlap. [g] Signals of the compound were not observed in DMSO and in DMSO/TFA (3/1).

**Scheme 4. Long-Range $^{1}H-^{15}N$ Coupling Constants Confirming the Structure of the Tetrazole (T and T′) Isomers of 2* and 4*[a]**

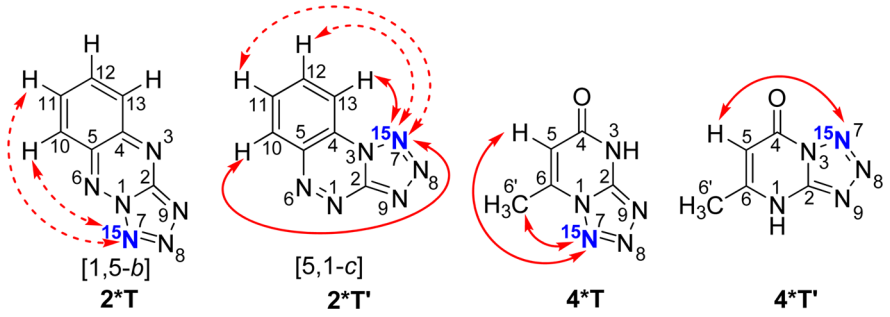


[a] The observed $^{1}H-^{15}N7$ $J$ coupling constants ($J_{HN}$) with magnitudes of $J \geq 0.1$ Hz and $J < 0.1$ Hz are indicated by the solid and dashed red arrows, respectively. The detection limits of the $J_{HN}$ measurements were 0.03 and 0.1 Hz (**2*** and **4***, respectively).

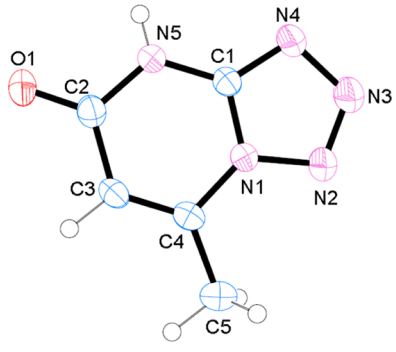


**Figure 3.** ORTEP diagram of the X-ray structure of compound **4T**.

$J_{HN}$-based methods to study heterocycle isomerization in solution.

## CONCLUSION

We have reported a new and effective NMR-based approach for the structural analysis of the azido-1,2,4-triazine and azidopyrimidine cyclization products. The selective incorporation of a $^{15}N$ label into the azolo core of the tetrazoloazines leads to the appearance of $^{1}H-^{15}N$ $J$ couplings, which can be easily measured in a quantitative fashion by using 1D spin−echo experiments. The analysis of the $J_{HN}$ coupling patterns allows for the unambiguous determination of the fusion type that occurs between the azole and azine rings in the cyclic forms (**T** and **T′**), even for the minor isomers, for which natural-abundance $^{13}C$ data are difficult to obtain. The proposed NMR


dx.doi.org/10.1021/jo4008207 | J. Org. Chem. 2013, 78, 6975−6982

methods could also be used to elucidate the molecular structures and chemical rearrangements in other nitrogen-containing heterocyclic compounds, especially when the application of conventional NMR techniques, which are based on the natural isotope abundances ($^1$H-COSY, $^{13}$C-/$^{15}$N-HMQC/HMBC, etc.), are problematic due to low proton and carbon densities.

## EXPERIMENTAL SECTION

**General Methods.** $Na^{15}NO_2$ (minimum 98% atom $^{15}$N) and the reagents for which the preparation is not described were obtained from commercial suppliers and used without further purification. $K^{15}NO_2$ with an 86% degree of $^{15}$N enrichment was prepared from $K^{15}NO_3$, according to a previously published protocol.[34]

**Instrumentation and Measurements.** High-resolution mass spectra (HRMS) were recorded on a linear ion trap LTQ-FT mass spectrometer with electrospray ionization (ESI). All NMR spectra were acquired by using a spectrometer that was equipped with a room-temperature triple-resonance ($^1$H, $^{13}$C, $^{15}$N) probe. The operating frequencies for $^1$H, $^{13}$C, and $^{15}$N were 700, 175, and 71 MHz, respectively. The measurements in the DMSO-$d_6$ solution and the DMSO-$d_6$/TFA-$d$ mixtures were performed at 42 °C (compound **2***) and 30 °C (compound **4***), respectively. The $^1$H chemical shifts were referenced to the residual $CD_2H$ signal of DMSO-$d_6$ at 2.51 ppm. The $^{13}$C and $^{15}$N chemical shifts were indirectly referenced to TMS and liquid $MeNO_2$, respectively.[37] When this indirect referencing scale was used, the $^{13}$C signal of DMSO-$d_6$ was observed at 40.11 ppm. The measurements in the TFA-$d$ solution were performed at 27 °C. In these cases, the $^{13}$C chemical shifts were referenced to the $^{13}$C signal of TFA-$d$ at 114.06 ppm.[34] The $^1$H and $^{15}$N chemical shifts were indirectly referenced by using ratios for TMS and liquid $MeNO_2$, respectively.[37]

The $^1$H, $^{13}$C, and $^{15}$N resonance assignments were performed by using gradient-enhanced versions of 2D $^1$H DQF COSY, $^{13}$C-HMQC, $^{13}$C-HMBC, and $^{15}$N-HMBC spectra (see the Supporting Information, Figures S2, S3, and S5). The 1D $^{13}$C spectra were recorded with broad-band or selective decoupling from the $^{15}$N nuclei, and the results of the $J_{CN}$ and $J_{HN}$ analysis were also used. In some cases, when the $J_{CN}$ and $J_{HN}$ data were not available due to the low concentrations of the isomeric forms, the assignments of the $^1$H and $^{13}$C resonances were based on a comparison between the spectra that were measured at various TFA concentrations.

The $J_{HN}$ couplings were detected and measured by using an amplitude-modulated spin−echo technique.[34,35] The $J$ coupling value was quantitatively extracted from the integral intensities of the multiplets in the 1D $^1$H spin−echo spectra, which were measured in an interleaved fashion with or without the selective inversion of the $^{15}$N nucleus of interest, in the middle of the echo period.[34] For the reference experiments, the inversion pulse was applied outside the studied spectral region. The B0 $z$ gradients were used to remove any imperfections that were associated with the $^1$H-refocusing and $^{15}$N-inversion pulses in the middle of the spin−echo. The antiphase $^1H_X{}^{15}N_Z$ magnetization was suppressed by broad-band $^{15}$N decoupling during acquisition.[34] The spin−echo delays $2 \times \Delta$ (the delay for the evolution of $J_{HN}$) were set to 2.0 and 0.6 s (compounds **2*** and **4***, respectively). In the last case, the use of shorter spin−echo delays was dictated by the fast transverse relaxation (broadening) of some of the **4*** $^1$H resonances. The spin−echo spectra that were used for the quantitative extraction of the $J_{HN}$ couplings were Fourier-transformed in absolute value mode to exclude any phase distortions that were created by homonuclear $^1$H−$^1$H $J$ couplings. The transverse relaxation rates ($R_2$) for a given $^1$H nucleus were assumed to be identical among the $^{15}$N-labeled and unlabeled variants of the compound. The following equation was used for the extraction of $J$ couplings:

$$J_{HN} = [\arccos I^C/I^D - (1 - a_i)/a_i]/2\pi\Delta \quad (1)$$

where $I^C$ (coupled) and $I^D$ (decoupled) are the intensities of the $^1$H multiplets measured *with* and *without* the selective inversion of the $^{15}$N nucleus, respectively, and $a_i$ is the degree of $^{15}$N enrichment (0.98 and 0.86 for **2*** and **4***, respectively).

Two methods were employed for the measurement of $J_{CN}$: amplitude-modulated 1D $^{13}$C spin−echo and $^{13}$C line-shape analysis.[34] In the first method, a 0.4 s spin−echo delay (the delay for the evolution of $J_{CN}$) was used. In the second method, the line shapes of the multiplets in the 1D $^{13}$C spectra, which were acquired with or without band-selective decoupling from the $^{15}$N nuclei, were fitted to the sum of several Lorentz lines.

The band-selective decoupling, band-selective inversion, and broad-band decoupling of the $^{15}$N nuclei were achieved by using WURST-20 adiabatic pulses[38] with a length of 20 ms and an inversion range of approximately 1 and 40 kHz (14 and 560 ppm on $^{15}$N).

**X-ray Crystallographic Analysis.** The diffraction data were collected on an X-ray diffractometer with Mo K$\alpha$ radiation ($\lambda$ = 0.71073 Å, graphite monochromator, $\omega/2\theta$-scanning technique). The structure was solved by direct methods that were implemented in the SHELXS-97 program.[39] The refinement was carried out through full-matrix anisotropic least-squares methods on $F^2$ for all reflections of the non-H atoms by using the SHELXL-97 program.[40] The X-ray CIF files are available in the Supporting Information and have been deposited at the Cambridge Crystallographic Data Centre and allocated with the deposition number CCDC 924927. Copies of the data can be obtained, free of charge, from the CCDC, 12 Union Road, Cambridge, CB2 1EZ U.K. (e-mail, deposit@ccdc.cam.ac.uk; web, www.ccdc.cam.ac.uk).

**Synthesis.** Compounds **1** and **3** were prepared according to previously published protocols.[41,42]

*[$^{15}$N]-Azidobenzo-1,2,4-triazine (**2*A**).* A solution of 3-hydrazinobenzo-1,2,4-triazine (**1**; 0.05 g, 0.31 mmol) in 1.00 mL of acetic acid was cooled to 0−5 °C, and aqueous $Na^{15}NO_2$ (0.028 g, 0.40 mmol in 0.4 mL of water) was added dropwise such that the temperature of the reaction mixture was maintained below 5 °C. The reaction mixture was stirred at room temperature for 30 min. The resulting precipitate was filtered and dried to yield compound **2*A** as a green solid (0.029 g, 54%): mp 116−117 °C; HMRS (ESI) $m/z$ calcd for $C_7H_5N_5{}^{15}N$ $[M + H]^+$ 174.0546, found 174.05406.

*[$^{15}$N]-Azidopyrimidine (**4*A**).* A solution of 2-hydrazino-6-methylpyrimidin-4-one (**3**; 0.10 g, 0.71 mmol) in 3.00 mL of acetic acid was cooled to 0−5 °C, and aqueous $K^{15}NO_2$ (0.08 g, 0.93 mmol in 1 mL of water) was added dropwise such that the temperature of the reaction mixture was maintained below 5 °C. After the mixture was stirred for 2 h at 5 °C, 10 mL of water was added. The resulting solution was extracted with ethyl acetate (3 × 5 mL). Evaporation of the solvent afforded compound **4*A** as a colorless solid (0.054 g, 50%): mp 240−242 °C; HMRS (ESI) $m/z$ calcd for $C_5H_6N_4{}^{15}NO$ $[M + H]^+$ 153.0542, found 153.05399.

## ASSOCIATED CONTENT

### Supporting Information

A CIF file and tables giving detailed crystallographic data for **4T** and figures giving 1D $^1$H and representative 2D $^{13}$C HMQC, 2D $^{13}$C HMBC, and 2D $^{15}$N HMBC spectra for compounds **2*** and **4***. This material is available free of charge via the Internet at http://pubs.acs.org.

## AUTHOR INFORMATION

### Corresponding Author

*E-mail for S.L.D.: deevsl@yandex.ru.

### Notes

The authors declare no competing financial interest.

## ACKNOWLEDGMENTS

This work was supported by the Federal Target Program "Scientific and Science-Educational Personnel of Innovative Russia" (State Contract No. 14.A18.21.0806) and the Russian

Foundation for Basic Research (Project Nos. 10-03-01007 and 12-03-31476).

## REFERENCES

(1) Cosyn, L.; Palaniappan, K. K.; Kim, S.-K.; Duong, H. T.; Gao, Z.-G.; Jacobson, K. A.; Van Calenbergh, S. *J. Med. Chem.* **2006**, *49*, 7373−7383.
(2) Gupte, A.; Boshoff, H. I.; Wilson, D. J.; Neres, J.; Labello, N. P.; Somu, R. V.; Xing, C.; Barry, C. E., III; Aldrich, C. C. *J. Med. Chem.* **2008**, *51*, 7495−7507.
(3) Lakshman, M. K.; Singh, M. K.; Parrish, D.; Balachandran, R.; Day, B. W. *J. Org. Chem.* **2010**, *75*, 2461−2473.
(4) Stengel, I.; Mishra, A.; Pootrakulchote, N.; Moon, S.-J.; Zakeeruddin, S. M.; Grätzel, M.; Bäuerle, P. *J. Mater. Chem.* **2011**, *21*, 3726−3734.
(5) Chamas, Z. E. A.; Guo, X.; Canet, J.-L.; Gautier, A.; Boyer, D.; Mahiou, R. *Dalton Trans.* **2010**, *39*, 7091−7097.
(6) Sylvers, L. A.; Wower, J. *Bioconjugate Chem.* **1993**, *4*, 411−418.
(7) Ramsinghani, S.; Koh, D. W.; Amé, J.-C.; Strohm, M.; Jacobson, M. K.; Slama, J. T. *Biochemistry* **1998**, *37*, 7801−7812.
(8) Shoemaker, M. T.; Haley, B. E. *Bioconjugate Chem.* **1996**, *7*, 302−310.
(9) Chattopadhyay, B.; Rivera Vera, C. I.; Chuprakov, S.; Gevorgyan, V. *Org. Lett.* **2010**, *12*, 2166−2169.
(10) Nilsson, L. I.; Ertan, A.; Weigelt, D.; Nolsöe, J. M. J. *J. Heterocycl. Chem.* **2010**, *47*, 887−892.
(11) Zhang, Q.; Wang, X.; Cheng, C.; Zhu, R.; Liu, N.; Hu, Y. *Org. Biomol. Chem.* **2012**, *10*, 2847−2854.
(12) Rykowski, A.; Van Der Plas, H. C.; Stam, C. H. *Acta Crystallogr.* **1977**, *B33*, 274−276.
(13) Dzimko, V. M.; Ivashchenko, A. V. *Chem. Heterocycl. Compd.* **1973**, *9*, 1082−1084.
(14) Lauria, A.; Diana, P.; Barraja, P.; Montalbano, A.; Cirrincione, G.; Dattolo, G.; Almerico, A. M. *Tetrahedron* **2002**, *58*, 9723−9727.
(15) Vinot, N.; Maitte, P. *J. Heterocycl. Chem.* **1986**, *23*, 721−725.
(16) Trust, R. I.; Albright, J. D.; Lovell, F. M.; Perkinson, N. A. *J. Heterocycl. Chem.* **1979**, *16*, 1393−1403.
(17) Shawali, A. S.; Gomha, S. M. *Tetrahedron* **2002**, *58*, 8559−8564.
(18) Smutin, V. Yu.; Gindin, V. A.; Sablina, N. O. *Chem. Heterocycl. Compd.* **2006**, *42*, 403−407.
(19) Pordeli, M. K. V.; Oksanich, V.; Chuiguk, V. A. *Chem. Heterocycl. Compd.* **1973**, *9*, 1166−1168.
(20) El Ashry, S. H. E.; Nadeem, S.; Shah, M. R.; Kilany, Y. E. *Adv. Heterocycl. Chem.* **2010**, *101*, 161−228.
(21) Hajós, G.; Messmer, A.; Neszmélyi, A.; Parkanyi, L. *J. Org. Chem.* **1984**, *49*, 3199−3203.
(22) Temple, C.; Coburn, W. C., Jr.; Thorpe, M. C., Jr.; Montgomery, J. A. *J. Org. Chem.* **1965**, *30*, 2395−2398.
(23) Goodman, M. M.; Atwood, J. L.; Carlin, R.; Hunter, W.; Paudler, W. W. *J. Org. Chem.* **1976**, *41*, 2860−2864.
(24) Tišler, M. *Synthesis* **1973**, 123−136.
(25) Goodman, M. M.; Paudler, W. W. *J. Org. Chem.* **1977**, *42*, 1866−1869.
(26) Castillón, S.; Vilarrasa, J. *J. Org. Chem.* **1982**, *47*, 3168−3169.
(27) Castillón, S.; Meléndze, E.; Pascual, C.; Vilarrasa, J. *J. Org. Chem.* **1982**, *47*, 3886−3890.
(28) Gourdain, S.; Petermann, C.; Martinez, A.; Harakat, D.; Clivio, P. *J. Org. Chem.* **2011**, *76*, 1906−1909.
(29) Messmer, A.; Hajós, G.; Tamás, J.; Neszmélyi, A. *J. Org. Chem.* **1979**, *44*, 1823−1825.
(30) Hull, W. E.; Künstlinger, M.; Breitmaier, E. *Angew. Chem.* **1980**, *92*, 957−959; *Angew. Chem., Int. Ed. Engl.* **1980**, *19*, 924−926.
(31) Thétaz, C.; Wehrli, F. W.; Wentrup, C. *Helv. Chim. Acta* **1976**, *59*, 259−264.
(32) Cmoch, P.; Stefaniak, L.; Webb, G. A. *Magn. Reson. Chem.* **1997**, *35*, 237−242.
(33) Cmoch, P. *Magn. Reson. Chem.* **2002**, *40*, 507−516.
(34) Deev, S. L.; Shenkarev, Z. O.; Shestakova, T. S.; Chupakhin, O. N.; Rusinov, V. L.; Arseniev, A. S. *J. Org. Chem.* **2010**, *75*, 8487−8497.
(35) Bax, A.; Vuister, G. W.; Grzesiek, S.; Delaglio, F.; Wang, A. C.; Tschudin, R.; Zhu, G. *Methods Enzymol.* **1994**, *239*, 79−105.
(36) Davis, D. G.; Agosta, W. C.; Cowburn, D. *J. Am. Chem. Soc.* **1983**, *105*, 6189−6190.
(37) Harris, R. K.; Becker, E. D.; Cabral de Menezes, S. M.; Goodfellow, R.; Granger, P. *Pure Appl. Chem.* **2001**, *73*, 1795−1818.
(38) Kupce, Ē.; Freeman, R. *J. Magn. Reson., Ser. A.* **1996**, *118*, 299−303.
(39) Sheldrick, G. M. *SHELXS-97, a Program for the Automatic Solution of Crystal Structures*; University of Göttingen, Göttingen, Germany, 1997.
(40) Sheldrick, G. M. *SHELXL-97, a Program for Crystal Structure Refinement*; University of Göttingen, Göttingen, Germany, 1997.
(41) Jiu, J.; Mueller, G. P. *J. Org. Chem.* **1959**, *24*, 813−818.
(42) Brady, L. E.; Herbst, R. M. *J. Org. Chem.* **1959**, *24*, 922−924.